Fabrication of $Y_2Si_2O_7$ coating and its oxidation protection for C/SiC composites

Qing-song MA, Li-hui CAI

National Key Laboratory of Advanced Ceramic Fibers and Composites,
National University of Defense Technology, Changsha 410073, China

Abstract: Yttrium silicate ($Y_2Si_2O_7$) coating was fabricated on C/SiC composites through dip-coating with silicone resin + Y_2O_3 powder slurry as raw materials. The synthesis, microstructure and oxidation resistance and the anti-oxidation mechanism of $Y_2Si_2O_7$ coating were investigated. $Y_2Si_2O_7$ can be synthesized by the pyrolysis of Y_2O_3 powder filled silicone resin at mass ratio of 54.2:45.8 and 800 °C in air and then heat treated at 1400 °C under Ar. The as-fabricated coating shows high density and favorable bonding to C/SiC composites. After oxidation in air at 1400, 1500 and 1600 °C for 30 min, the coating-containing composites possess 130%−140% of original flexural strength. The desirable thermal stability and the further densification of coating during oxidation are responsible for the excellent oxidation resistance. In addition, the formation of eutectic Y−Si−Al−O glassy phase between $Y_2Si_2O_7$ and Al_2O_3 sample bracket at 1500 °C is discovered.
Key words: C/SiC composites; yttrium silicate; coating; oxidation resistance

1 Introduction

Continuous carbon fiber reinforced silicon carbide (C/SiC) composites have been considered as a kind of strategic thermostructural materials for hypersonic vehicles and high performance engines because of several advantages such as high specific strength and modulus, high damage tolerance, excellent thermal stability, and desirable corrosion resistance [1,2]. However, there are some pores and microcracks in C/SiC composites inevitably due to intrinsic characteristics of fabrication technologies such as precursor infiltration and pyrolysis (PIP) and chemical vapor infiltration (CVI) and the coefficient of thermal expansion (CTE) mismatch between fiber and matrix [3]. The existence of pores and microcracks makes it easy for oxygen to diffuse into C/SiC composites and then oxidize carbon fiber. Some measures including fiber coating, matrix modification and external coating have been adopted to protect C/SiC composites from oxidation in which external coating is demonstrated to be the most effective method [4−7].

Yttrium silicate ($Y_2Si_2O_7$ and Y_2SiO_5) is a desirable candidate for external coating and has been investigated extensively for oxidation protection of C/C and C/SiC composites owing to high melt point, low oxygen permeability accompanied with favorable thermal and chemical stability, low modulus and suited CTE [8−14]. Several processes have been employed to prepare yttrium silicate external coating. The main fabrication routes include plasma spray [8], electrophoretic deposition [9], sol−gel [10], slurry brushing and sintering [11,12], and so on.

Recently, the synthesis of yttrium silicate by the pyrolysis of Y_2O_3 powder filled silicone resin has been reported [13,14]. This novel route is a potential method due to good adhesive and covering ability of silicone resin, ability to coat complex structures, low process temperature, and relative low cost [15]. Dense and thick $Y_2Si_2O_7$ coatings were manufactured on SiC foam in Ref. [13] by thermal treatment of silicone resin containing Y_2O_3 nano-sized powders in air, but the oxidation protection for C/SiC composites was not carried out. In Ref. [14], $Y_2Si_2O_7$ coating derived from silicone resin containing Y_2O_3 micro-sized powders

exhibited good oxidation protection for C/SiC composites at 1400 °C. However, there were some free carbon and pores in coating because the pyrolysis of silicone resin was performed under inert atmosphere, which is detrimental to oxidation resistance at high temperatures. In this study, micro-sized Y_2O_3 powder filled silicone resin was pyrolyzed in air to prepare $Y_2Si_2O_7$ coating on C/SiC composites, and the anti-oxidation property of coating was investigated.

2 Experimental

C/SiC composites with an apparent density of 1.92 g/cm^3 and an open porosity of 9.75% were fabricated by PIP route. The silicone resin with a trademark of DC249 and the Y_2O_3 powders with a diameter of 2−3 μm and a purity of 99.99% were selected to synthesize $Y_2Si_2O_7$. The mass ratio of Y_2O_3 to DC249 was set to be 54.2:45.8 according to the composition of $Y_2O_3 \cdot 2SiO_2$ and ceramic yield (~63%) of DC249 in air.

The silicone resin was dissolved in anhydrous ethanol, to which Y_2O_3 powders were added. After being stirred for 4 h, the slurry was obtained. For the synthesis of $Y_2Si_2O_7$, the slurry was dried at 100 °C for 6 h, followed by cross-linking at 250 °C for 2 h. The cured sample was pyrolyzed in air at 800 °C, and then heated under flowing high purity argon at 1200, 1300, and 1400 °C, respectively. TG−DSC measurement was performed on a thermogravimetric analyzer (NETZSCH STA 429 CD) with a heating rate of 10 °C/min to investigate thermal decomposition behavior of the cured sample. X-ray diffraction (XRD) measurements were carried out on a diffractometer (D/max−2400, Rigaku) with Cu K$_\alpha$ radiation. Data were digitally recorded during a continuous scan in 2θ range from 10° to 60° with a scanning rate of 4 (°)/min.

The preparation of $Y_2Si_2O_7$ coating included three steps, namely, dip-coating, pre-pyrolysis and heat treatment. In the first step, C/SiC composite substrate was dipped in slurry for 5 min, then drawn out of slurry with a constant speed and dried at 80 °C for 1 h. After repeating 4 times of dip-coating process, C/SiC composite substrate was heated at 250 °C for 2 h to cure silicone resin, followed by pyrolysis at 800 °C for 1 h in air to convert silicone resin into SiO_2. The process consisting of dip-coating (4 times) and pre-pyrolysis was repeated 3 times. Finally, the coated C/SiC composites were obtained after being heated at 1400 °C for 1 h under flowing high purity argon. The as-received coated C/SiC composites were placed on Al_2O_3 bracket in muffle and oxidized at 1400, 1500 and 1600 °C for 30 min, respectively. The mass loss and the flexural strength retention after oxidation were recorded to

characterize the oxidation resistance of $Y_2Si_2O_7$ coating. To elucidate the anti-oxidation mechanism, scanning electron microscope (SEM) equipped with energy dispersive spectroscopy (EDS) (Quanta−200 EDAX) and XRD were employed to observe the changes of microstructure, element and phase of coating after oxidation.

3 Results and discussion

3.1 Synthesis of $Y_2Si_2O_7$

The thermal decomposition curve of cured silicone resin containing Y_2O_3 powders in air is shown in Fig. 1. There is a mass loss of ~1% from room temperature to 180 °C, which is related to the volatilization of residual ethanol. As a result, the endothermic peak at 90 °C appears. When temperature is elevated to 520 °C, another ~2% mass loss occurs. This can be explained by the further condensation of Si—OH radicals and the decomposition of species with low relative molecule mass. As can be seen from Fig. 1, the major mass loss of ~14% occurs from 520 to 800 °C accompanied by two exothermic peaks at ~670 and ~720 °C, which is corresponding to the chemical bond cracking and redistribution reaction of silicone resin in oxidative atmosphere. At temperatures exceeding 800 °C, no obvious mass loss and caloric change are observed, indicating the completion of pyrolysis of silicone resin.
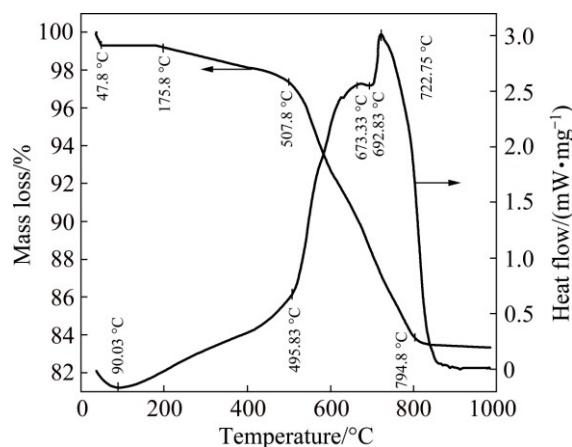

Fig. 1 TG−DSC curves of cured silicone resin containing Y_2O_3 powders

Figure 2 shows the XRD patterns of cured silicone resin containing Y_2O_3 powders pyrolyzed at different temperatures. According to the results of FTIR and XRD [16], the pyrolyzate of silicone resin in air is amorphous SiO_2. Therefore, there are only diffraction peaks of Y_2O_3 at 800 °C. Obvious diffraction peaks of $Y_2Si_2O_7$ emerge at 1200 °C, suggesting that the reaction between Y_2O_3 and SiO_2 takes place at this temperature. With increasing temperature, the diffraction peaks of

$Y_2Si_2O_7$ become more and more intense while those of Y_2O_3 are gradually faint. At 1400 °C, all peaks can be assigned to yttrium silicate, implying that the reaction between Y_2O_3 and SiO_2 is basically finished. It is noted that there are some diffraction peaks of Y_2SiO_5 existing in the XRD pattern at 1400 °C. This may be explained by two reasons. One is a slight deviation of mass ratio of Y_2O_3 to silicone resin from the stoichiometric ratio of Y_2O_3 to SiO_2 due to the fluctuation of ceramic yield of silicone resin in air. The other is that mixture uniformity is not good enough.

3.2 Oxidation resistance of $Y_2Si_2O_7$ coating

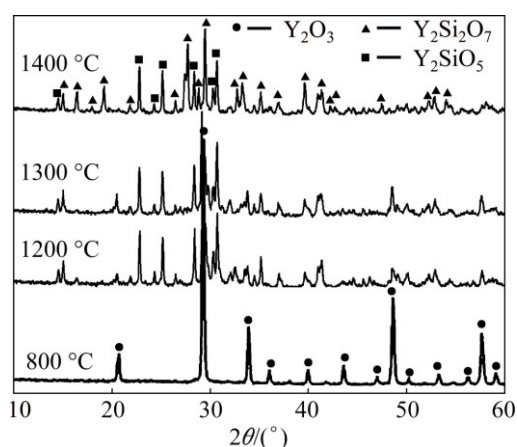Figure 3 displays the SEM images of as-received

Fig. 2 XRD patterns of cured silicone resin containing Y_2O_3 powders pyrolyzed at different temperatures
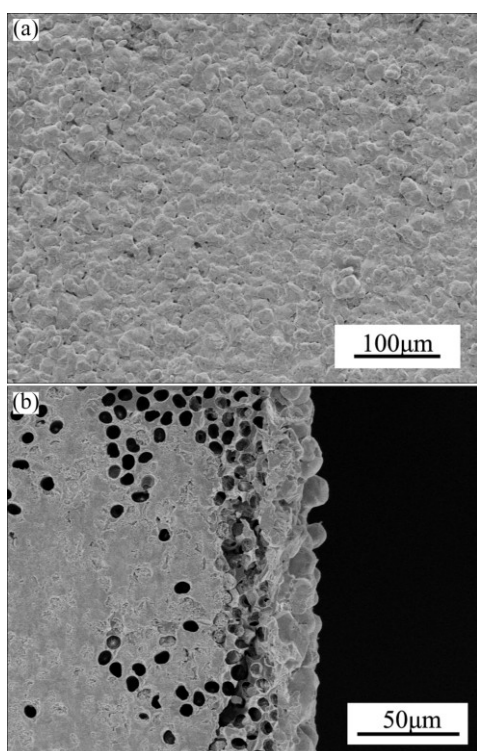

Fig. 3 SEM images of surface (a) and cross section (b) of as-received coating

$Y_2Si_2O_7$ coating. As shown in Fig. 3, the coating is uniform and compact as a whole with a few pores. As a result of favorable CTE match between $Y_2Si_2O_7$ coating and C/SiC composite substrate, no cracks are observed on surface and cross-section. Nevertheless, some cavities resulting from oxidation of some carbon fibers can be seen on cross-section, which is found to impair the flexural strength of C/SiC composite substrate. When silicone resin was decomposed in air at 800 °C, C/SiC composites were prone to oxidation at the same time due to not fully compact coating. This problem will be focused in subsequent research by means of introducing a layer of anti-oxidation coating.

After being oxidized at 1400, 1500 and 1600 °C for 30 min, the mass loss and the mechanical properties retention of the coated C/SiC composites are listed in Table 1. From the viewpoint of mass loss, the coated composites exhibit tiny mass loss after oxidation at 1400 and 1500 °C. As for the mass loss of 3.47% at 1600 °C, it is not actual and will be explained in detail in Section 3.3. From the viewpoint of mechanical properties retention, the flexural strength and modulus are not decreased after oxidation and remarkably enhanced on the contrary. It is found that the flexural strength is increased by 30%−40% after oxidation and the modulus is increased by 5%−30% from 1400 to 1600 °C. In all, the data show that the $Y_2Si_2O_7$ coating provides excellent oxidation protection for C/SiC composites.

Table 1 Mass change and mechanical properties retention of $Y_2Si_2O_7$-coated C/SiC composites after oxidation

Oxidation temperature/°C	Mass change/%	Flexural strength retention/%	Flexural modulus retention/%
1400	0	143.4	105.5
1500	−0.69	144.3	120.3
1600	−3.47	129.8	131.0

Figures 4 and 5 present load−displacement curves and fracture surfaces of the coated C/SiC composites before and after oxidation, respectively. As shown in Fig. 4, all coated composites illustrate non-catastrophic fracture behavior with the maximum displacement of ~1 mm at invalidation point. It is clear from Fig. 5 that all the coated composites show extensive fiber pull-out and long pull-out length, which corresponds with the load−displacement curves. In combination with the data in Table 1, it is indicated that $Y_2Si_2O_7$ coating is a desirable candidate of anti-oxidation for C/SiC composites. Although there are some degradations in flexural strength during fabrication, $Y_2Si_2O_7$ coating protects C/SiC composites from being damaged during oxidation. Apart from similarity, there are some
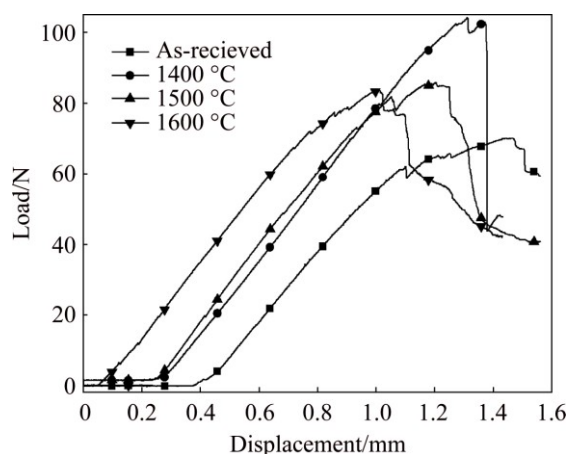
Fig. 4 Load−displacement curves of Y₂Si₂O₇-coated C/SiC composites before and after oxidation

differences in Figs. 4 and 5. It can be found from Fig. 4 that the slope of 1500 °C curve, which is almost the same as that of 1600 °C curve, is a little higher than that of 1400 °C curve which is approximately equal to that of original curve. This is in accordance with the data of flexural modulus retention in Table 1 and can be ascribed to the improvement in density of coating. In addition, the 1400 °C curve shows vertical decline after invalidation point, and the rest exhibits zigzag decline on the contrary.

In the top half of Fig. 5(b), relatively flat fracture surface is found, which is responsible for the vertical decline of 1400 °C curve. However, the reason for this phenomenon is not clear at present. Maybe, it is just a reflection of the inherent non-uniformity of ceramic matrix composites.

3.3 Anti-oxidation mechanism of $Y_2Si_2O_7$ coating

To elucidate the anti-oxidation mechanism, XRD patterns and surface morphologies of $Y_2Si_2O_7$ coatings before and after oxidation were recorded and presented in Figs. 6 and 7, respectively. In Fig. 6, there is scarcely any discrepancy among the patterns, implying that $Y_2Si_2O_7$ coating has good thermal stability at the temperatures ranging from 1400 to 1600 °C. At the same time, the coating is considered to have good chemical compatibility with composite substrate and ambient atmosphere due to no emergence of other diffraction peaks of new phases.

Figure 7(a) shows original surface of as-fabricated coating, displaying some microcracks and pores. In the small picture at top right corner, the microcracks and pores are obvious and the claylike microstructure can be observed. After oxidation at 1400 °C for 30 min, there are no obvious changes on coating surface as a whole. However, sinter-like microstructure is clearly seen from the small picture at top right corner of Fig. 7(b),
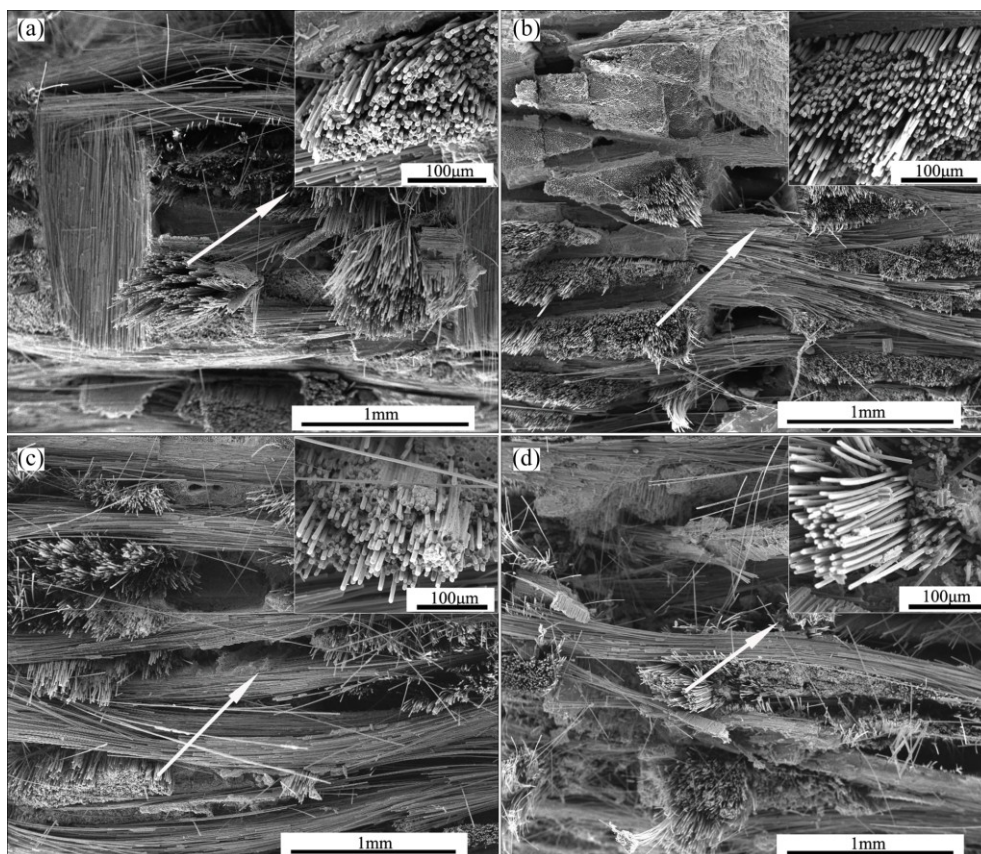

Fig. 5 SEM images of fracture surfaces of Y₂Si₂O₇-coated C/SiC composites: (a) Before oxidation; (b) After oxidation at 1400 °C for 30 min; (c) After oxidation at 1500 °C for 30 min; (d) After oxidation at 1600 °C for 30 min
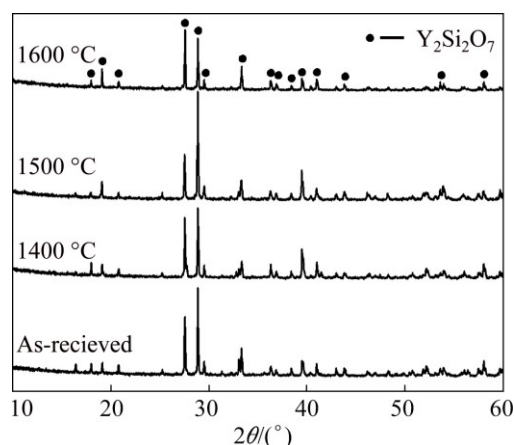
Fig. 6 XRD patterns of $Y_2Si_2O_7$ coatings before and after oxidation

demonstrating the occurrence of further densification of $Y_2Si_2O_7$ coating during oxidation. With increasing oxidation temperature, further densification is intensified. As illustrated in Figs. 7(c) and (d), the microcracks and pores are diminished gradually, leading to more and more compacted coating. By comparing the small pictures at top right corner of Figs. 7(b)−(d), further densification can be seen more clearly. The viscous flow of glassy phase and the solid-state sintering of $Y_2Si_2O_7$ are proposed to be responsible for the healing of microcracks and pores.

Figure 8 and Table 2 show surface morphologies

and EDS results of $Y_2Si_2O_7$ coating in contact with Al_2O_3 bracket after oxidation. Similarly, the coating in contact with Al_2O_3 bracket becomes more and more compacted with increasing oxidation temperature. However, it can be observed that the coating in contact with Al_2O_3 bracket presents more densified state at the same oxidation temperature, especially at 1500 and 1600 °C, by comparing Figs. 7(b)−(d) with Figs. 8(a)−(c), respectively.

Table 2 shows the relative content change of coating element as a function of oxidation temperature. Gradual decrease of O and Y elements and increase of Si element are observed. It is noteworthy that the relative content of Y element is dramatically reduced and Al element is detected when temperature is elevated from 1500 to 1600 °C. This can be ascribed to the formation of glassy Y−Si−Al−O eutectic phase from the reaction of $Y_2Si_2O_7$ coating and Al_2O_3 bracket [17]. In the work of HUANG et al [8], it was confirmed that the reaction took place at 1500 °C.

Since the melting point of Y−Si−Al−O phase is about 1400 °C [18], the microcracks and pores in as-received coating can be healed by the viscous flow of glassy Y−Si−Al−O phase at 1500 and 1600 °C, leading to more compacted coating. However, local desquamation of coating is observed when the sample is taken away from Al_2O_3 bracket, as shown in Figs. 8(b) and (c), which is due to the adhesive effect of glassy Y−Si−Al−O phase. Therefore, the obvious mass loss and
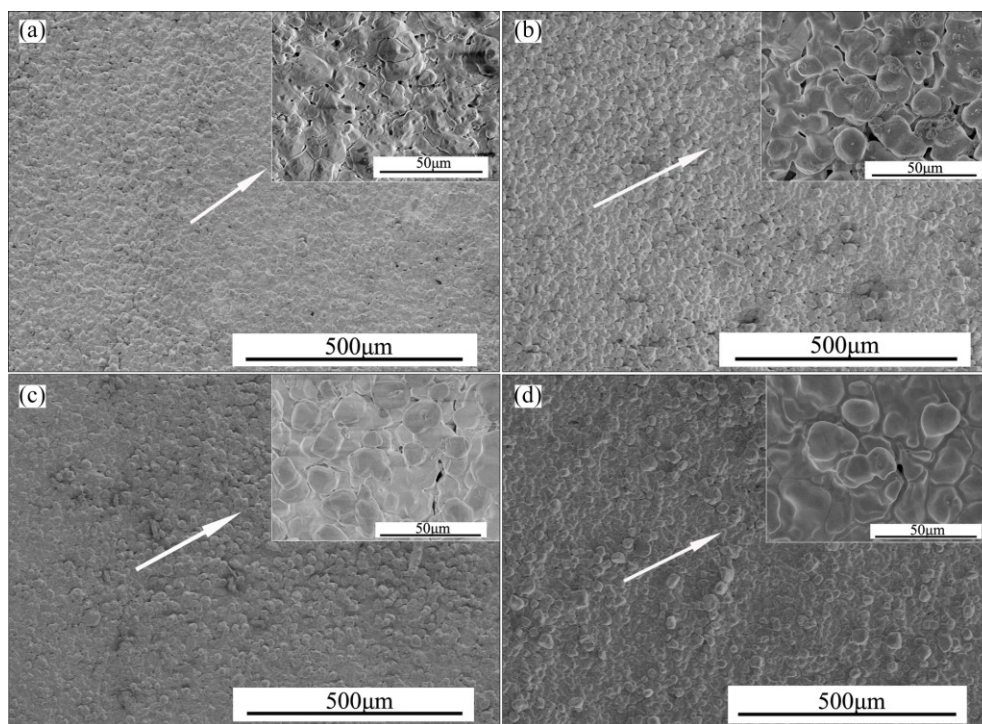

Fig. 7 SEM images of $Y_2Si_2O_7$ coatings: (a) Before oxidation; (b) After oxidation at 1400 °C for 30 min; (c) After oxidation at 1500 °C for 30 min; (d) After oxidation at 1600 °C for 30 min
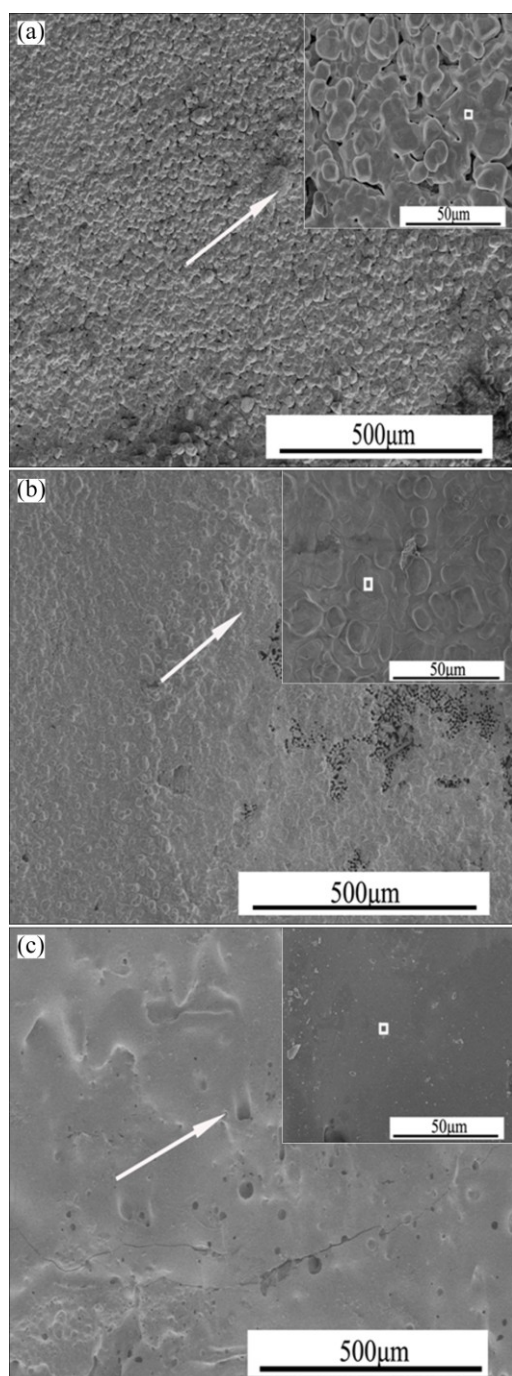
Fig. 8 SEM images of $Y_2Si_2O_7$ coatings in contact with Al_2O_3 bracket: (a) After oxidation at 1400 °C for 30 min; (b) After oxidation at 1500 °C for 30 min; (c) After oxidation at 1600 °C for 30 min

Table 2 EDS results of $Y_2Si_2O_7$ coating in contact with Al_2O_3 bracket after oxidation

Oxidation temperature/°C	Mole fraction/%			
	O	Si	Y	Al
1400	67.67	17.44	14.89	−
1500	63.58	21.67	14.75	−
1600	61.61	31.33	3.51	3.55

EDS was carried out in white pane in Fig. 8

the lower flexural strength retention at 1600 °C are owing to local desquamation of coating instead of oxidation of C/SiC composites, demonstrating the excellent oxidation protection of $Y_2Si_2O_7$ coating itself at this temperature.

In a word, the $Y_2Si_2O_7$ coating shows excellent oxidation resistance as a result of high density and desirable thermal and chemical stability at high temperatures. At the same time, the resistance to crack creation and propagation of composite surface is reinforced due to further densification of coating, thus improving mechanical properties of C/SiC composites.

4 Conclusions

1) When the mass ratio of Y_2O_3 powder to silicone resin is 54.2:45.8, yttrium silicate ($Y_2Si_2O_7$) can be synthesized by pyrolysis at 800 °C in air and then heat treatment at 1400 °C under Ar.

2) $Y_2Si_2O_7$ coating with high density and favorable bonding to C/SiC substrate was prepared by dip-coating. The coated C/SiC composites possess 143.4%, 144.3% and 129.8% of original flexural strength after being oxidized at 1400, 1500 and 1600 °C for 30 min, respectively.

3) Desirable thermal stability and further densification during high temperature oxidation result in excellent oxidation resistance of $Y_2Si_2O_7$ coating.

References

[1]   NASLAIN R. Design, preparation and properties of non-oxide CMCs for application in engines and nuclear reactors: An overview [J]. Composites Science and Technology, 2004, 64: 155−170.

[2]   MA Qing-song, LIU Hai-tao, PAN Yu, LIU Wei-dong, CHEN Zhao-hui. Research progress on the application of C/SiC composites in scramjet [J]. Journal of Inorganic Materials, 2013, 28(3): 248−255. (in Chinese)

[3]   LI Wei, CHEN Zhao-hui. Pore geometry of 3D-C$_f$/SiC composites by mercury intrusion porosimetry [J]. Ceramics International, 2009, 35(2): 747−753.

[4]   XIANG Yang, LI Wei, WANG Song, CHEN Zhao-hui. Oxidation behavior of oxidation protective coatings for PIP-C/SiC composites at 1500 °C [J]. Ceramics International, 2012, 38(1): 9−13.

[5]   SUN Can, LI He-jun, FU Qian-gang, ZHANG Jia-ping, PENG Han. Double SiC coating on carbon/carbon composites against oxidation by a two-step method [J]. Transactions of Nonferrous Metals Society of China, 2013, 23: 2107−2112.

[6]   HUANG Dong, ZHANG Ming-yu, HUANG Qi-zhong, WANG Li-ping, TANG Xian, YANG Xin, TONG Kai. Fabrication and ablation property of carbon/carbon composites with novel SiC−ZrB$_2$ coating [J]. Transactions of Nonferrous Metals Society of China, 2015, 25: 3708−3715.

[7]   FU Qian-gang, ZHANG Jia-ping, ZHANG Zheng-zhong, LI He-jun, SUN Can. SiC−MoSi$_2$/ZrO$_2$−MoSi$_2$ coating to protect C/C composites against oxidation [J]. Transactions of Nonferrous Metals Society of China, 2013, 23: 2113−2117.

[8] HUANG Jian-feng, LI He-jun, ZENG Xie-rong, LI Ke-zhi, XIONG Xin-bo, HUANG Min, ZHANG Xiu-lian, LIU Ying-lou. A new SiC/yttrium silicate/glass multi-layer oxidation protective coating for carbon/carbon composites [J]. Carbon, 2004, 42: 2356−2359.

[9] ARGIRUSIS C, DAMJANOVIĆ T, BORCHARDT G. Yttrium silicate coating system for oxidation protection of C/C−Si−SiC composites: Electrophoretic deposition and oxygen self-diffusion measurements [J]. Journal of the European Ceramic Society, 2007, 27: 1303−1306.

[10] APARICIO M, DURÁN A. Preparation and characterization of $50SiO_2−50Y_2O_3$ sol−gel coatings on glass and SiC(C/SiC) composites [J]. Ceramics International, 2005, 31: 631−634.

[11] HUANG Jian-feng, LI He-jun, ZENG Xie-rong, DENG Fei, XIONG Xin-bo, LI Ke-zhi. Oxidation resistant yttrium silicates coating for carbon/carbon composites prepared by a novel in-situ formation method [J]. Ceramics International, 2007, 33: 887−890.

[12] ZHENG Xiao-hui, DU Yong-guo, XAIO Jia-yu, LU Yu-feng, LIANG Chi-yong. Celsian/yttrium silicate protective coating prepared by microwave sintering for C/SiC composites against oxidation [J]. Materials Science and Engineering A, 2009, 505(1−2): 187−190.

[13] BERNARDO E, PARCIANELLO G, COLOMBO P. Novel synthesis and applications of yttrium silicates from a silicone resin containing oxide nano-particle fillers [J]. Ceramics International, 2012, 38: 5469−5474.

[14] LIU Jia, ZHANG Li-tong, HU Fei, YANG Juan, CHENG Lai-fei, WANG Yi-guang. Polymer-derived yttrium silicate coatings on 2D C/SiC composites [J]. Journal of the European Ceramic Society, 2013, 33: 433−439.

[15] LIU Jia, ZHANG Li-tong, LIU Qiao-mu, CHENG Lai-fei, WANG Yi-guang. Polymer-derived SiOC-BSAS coatings as an environmental barrier for C/SiC composites [J]. Journal of the American Ceramic Society, 2010, 93(12): 4148−4152.

[16] MA Qing-song, MA Yan, CHEN Zhao-hui. Fabrication and characterization of nanoporous SiO_2 ceramics via pyrolysis of silicone resin filled with nanometer SiO_2 powders [J]. Ceramics International, 2010, 36: 2269−2272.

[17] HWANG S L, CHEN I W. Reaction hot pressing of $α'$- and $β'$-Sialon ceramics [J]. Journal of the American Ceramic Society, 1994, 77(1): 165−171.

[18] LEE K N, FOX D S, BANSAL N P. Rare earth silicate environmental barrier coatings for SiC/SiC composites and Si_3N_4 ceramics [J]. Journal of the European Ceramic Society, 2005, 25: 1705−1715.

$Y_2Si_2O_7$ 涂层的制备及其对 C/SiC 复合材料的氧化保护作用

马青松，蔡利辉

国防科技大学　新型陶瓷纤维及其复合材料国家重点实验室，长沙 410073

摘　要：以 Y_2O_3 粉和硅树脂配制成的浆料为原料，通过浸涂提拉法在 C/SiC 复合材料表面制备 $Y_2Si_2O_7$ 涂层，研究 $Y_2Si_2O_7$ 相的合成、涂层结构和氧化保护效果以及抗氧化机制。结果表明，质量比为 54.2:45.8 的 Y_2O_3 粉/硅树脂混合物先在 800 ℃ 空气中裂解再在 1400 ℃ Ar 惰性气氛下热处理，能够完全转化成 $Y_2Si_2O_7$。$Y_2Si_2O_7$ 涂层致密度高且与基体结合紧密，在氧化过程中发生进一步致密化而呈现出优异的抗氧化性能，分别在 1400、1500 和 1600 ℃ 氧化 30 min 后，复合材料的强度保留率达到 130%~140%。此外，在 1500 ℃ 下 $Y_2Si_2O_7$ 涂层会与氧化铝支撑体之间发生反应，生成具有低共熔点的 Y−Si−Al−O 玻璃相。
关键词：C/SiC 复合材料；硅酸钇；涂层；抗氧化性

(Edited by Wei-ping CHEN)